Title: Principles for implicit integration

Author(s): Burby, Joshua William

Intended for: Internal LANL seminar

Issued: 2021-06-09

Principles for implicit integration

J. W. Burby (LANL, T-5)

July 9th, 2021
CNLS Seminar

Explicit integration usually timestep limited by numerical stability

$$\dot{x} = -\gamma\, x, \quad \gamma \in \mathbb{R}_+$$

Explicit integration usually timestep limited by numerical stability

$$\frac{x_{n+1} - x_n}{h} = -\gamma\, x_n$$

Explicit integration usually timestep limited by numerical stability

$$x_n = (1 - h\,\gamma)^n\,x_0$$

Explicit integration usually timestep limited by numerical stability

$$x_n = (1 - h\,\gamma)^n\, x_0$$

Numerical instability when $h\,\gamma > 2$

Implicit integration removes this stability barrier.

$$\frac{x_{n+1} - x_n}{h} = -\gamma\, x_{n+1}$$

Implicit integration removes this stability barrier.

$$x_n = \frac{1}{(1 + h\,\gamma)^n}\,x_0$$

Implicit integration removes this stability barrier.

$$x_n = \frac{1}{(1 + h\,\gamma)^n}\, x_0$$

Stable for all (non-negative) timesteps h!

But stability does not imply large timestep accuracy!

$$\frac{x_{n+1} - x_n}{h} = -\gamma\, x_{n+1} - h^4\, \gamma^5\, (x_{n+1} - 5)$$

Same formal accuracy as BWD Euler for $h\,\gamma \ll 1$

But stability does not imply large timestep accuracy!

$$x_n = \frac{x_0}{(1 + h\,\gamma + h^5\,\gamma^5)^n} + 5\left(\frac{h^5\,\gamma^5}{1 + h\,\gamma + h^5\,\gamma^5}\right)\frac{1 - (1 + h\,\gamma + h^5\,\gamma^5)^{-n}}{1 - (1 + h\,\gamma + h^5\,\gamma^5)^{-1}}$$

But stability does not imply large timestep accuracy!

$$x_n = \frac{x_0}{(1 + h\,\gamma + h^5\,\gamma^5)^n} + 5\left(\frac{h^5\,\gamma^5}{1 + h\,\gamma + h^5\,\gamma^5}\right)\frac{1 - (1 + h\,\gamma + h^5\,\gamma^5)^{-n}}{1 - (1 + h\,\gamma + h^5\,\gamma^5)^{-1}}$$
$$\approx 5h^4\,\gamma^4 \ll 1 \quad \text{as } n \to \infty$$

When $h\,\gamma \ll 1$, reasonable large-n behavior

But stability does not imply large timestep accuracy!

$$x_n = \frac{x_0}{(1 + h\,\gamma + h^5\,\gamma^5)^n} + 5\left(\frac{h^5\,\gamma^5}{1 + h\,\gamma + h^5\,\gamma^5}\right)\frac{1 - (1 + h\,\gamma + h^5\,\gamma^5)^{-n}}{1 - (1 + h\,\gamma + h^5\,\gamma^5)^{-1}}$$

$$\approx 5 \quad \text{as } n \to \infty$$

When $h\,\gamma \gg 1$, nonsensical large-n behavior

Large timesteps: a leap of faith?

Large timesteps: a leap of faith?

How can one step over timescales without sacrificing accuracy?

This talk will suggest an answer.

(1) Identify your c^{ts}-time system's temporal multi-scale structure

(2) Develop a discrete-time analogue of that structure

(3) Design implicit scheme using discrete structure as a constraint

This talk will suggest an answer.

Why?

(1) Develop a precise picture of interplay between short and long timescales in c$^{\text{ts}}$ time

(2) Understand how much of that interplay is reproducible in discrete time

(3) Use c$^{\text{ts}}$-time analytical methods for numerical analysis

Part I: fast-slow maps

Fast-slow systems embody most fundamental multi-scale structure

Definition 1: (fast-slow system)

A **fast-slow system** is a (possibly infinite-dimensional) ODE on $X \times Y \ni (x, y)$ of the form

$$\begin{aligned} \dot{y} &= f_\epsilon(x, y) \\ \dot{x} &= \epsilon\, g_\epsilon(x, y), \end{aligned}$$

where $f_\epsilon(x, y), g_\epsilon(x, y)$ are smooth in (x, y, ϵ) and

- For each x there is a unique $y = y_0^*(x)$ that solves $f_0(x, y) = 0$
- The linear map $D_y f_0(x, y_0^*(x)) : Y \to Y$ is invertible for each $x \in X$

x is slow variable, y is fast variable

Different limiting fast-variable phase portraits

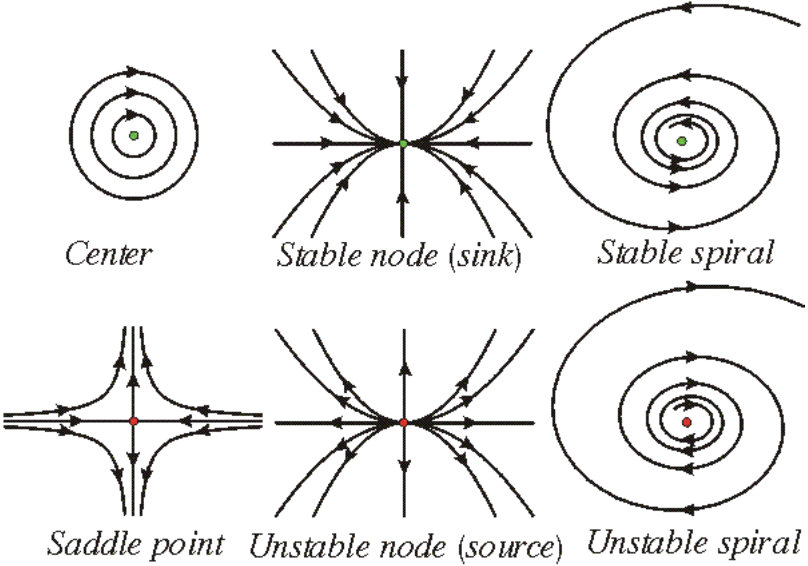

Fast-slow structure $\Rightarrow$ existence of slow manifold

Theorem 1: (existence of slow manifolds; c^{ts}-time)

- For each fast-slow system there is a unique formal power series

$$y_\epsilon^*(x) = y_0^*(x) + \epsilon\, y_1^*(x) + \epsilon^2\, y_2^*(x) + \ldots$$

  such that the graph $S_\epsilon = \{(x, y) \mid y = y_\epsilon^*(x)\}$ is an invariant manifold *to all orders in* ϵ.

- Equivalently, $y = y_\epsilon^*(x)$ provides a formally-exact closure of the slow-variable evolution equations,

$$\dot{x} = \epsilon\, g_\epsilon(x, y_\epsilon^*(x)).$$

Slow manifold reduction of the fast-slow system

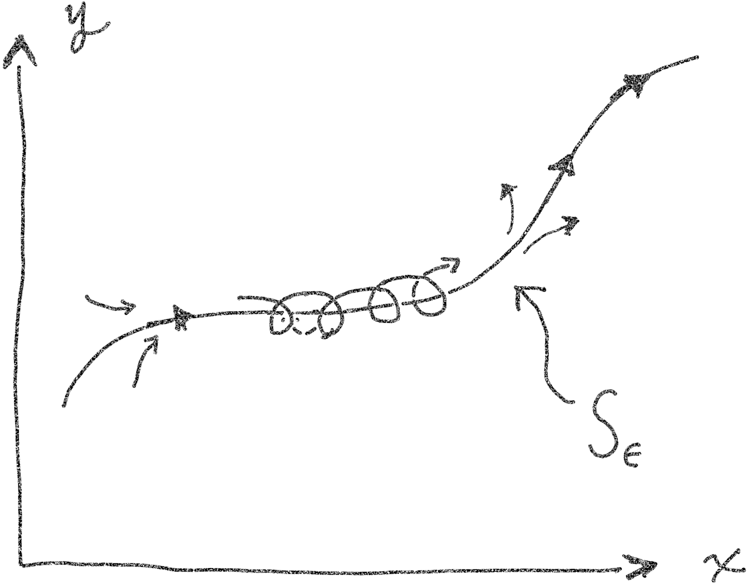
y
x
S_ϵ

Example:

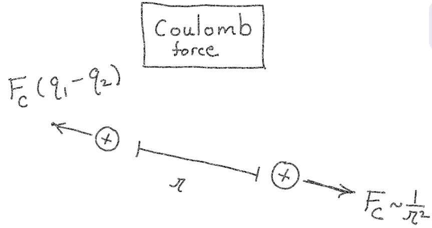

The Vlasov-Poisson system

$$\partial_t f + \boldsymbol{v} \cdot \nabla f + \tfrac{e}{m} \boldsymbol{F} \cdot \nabla_{\boldsymbol{v}} f = 0$$

$$\boldsymbol{F} = -\nabla \phi, \quad \Delta \phi = -4\pi e \int f \, d^3\boldsymbol{v}$$

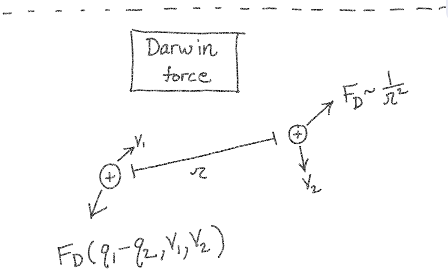

The Vlasov-Darwin system

$$\partial_t f + \boldsymbol{v} \cdot \nabla f + \frac{e}{m} \boldsymbol{a} \cdot \nabla_{\boldsymbol{v}} f = 0$$

$$\boldsymbol{F} = -\nabla \phi - c^{-1} \partial_t \boldsymbol{A}$$
$$+ c^{-1} \boldsymbol{v} \times \nabla \times \boldsymbol{A}$$

$$\Delta \phi = -4\pi e \int f \, d^3\boldsymbol{v} - c^{-1} \nabla \cdot \partial_t \boldsymbol{A}$$

$$c \nabla \times \nabla \times \boldsymbol{A} = 4\pi \int \boldsymbol{v} \, f d^3\boldsymbol{v} - \nabla \partial_t \phi$$

Example:

The Vlasov-Maxwell system

$$\partial_t f + \boldsymbol{v}\cdot\nabla f + \tfrac{e}{m}\boldsymbol{F}\cdot\nabla_{\boldsymbol{v}} f = 0$$
$$\boldsymbol{F} = \boldsymbol{E} + c^{-1}\boldsymbol{v}\times\boldsymbol{B}$$
$$\partial_t \boldsymbol{B} = -c\nabla\times\boldsymbol{E}$$
$$\partial_t \boldsymbol{E} = 4\pi\int \boldsymbol{v}\, f\, d^3\boldsymbol{v} - c\,\nabla\times\boldsymbol{B}$$

- Fast-slow with $x = (f, \boldsymbol{E}_L)$, $y = (\boldsymbol{B}, \boldsymbol{E}_T)$, $\epsilon = c^{-1}$
- Vlasov-Poisson is 0^{th}-order slow manifold reduction
- Vlasov-Darwin is 1^{st}-order slow manifold reduction

G. Miloshevich and J. W. Burby, *J. Plasma Phys.* (2021, in-press)

The Vlasov-Poisson system

$$\partial_t f + \boldsymbol{v}\cdot\nabla f + \tfrac{e}{m}\boldsymbol{F}\cdot\nabla_{\boldsymbol{v}} f = 0$$
$$\boldsymbol{F} = -\nabla\phi, \quad \Delta\phi = -4\pi e\int f\, d^3\boldsymbol{v}$$

The Vlasov-Darwin system

$$\partial_t f + \boldsymbol{v}\cdot\nabla f + \frac{e}{m}\boldsymbol{a}\cdot\nabla_{\boldsymbol{v}} f = 0$$
$$\boldsymbol{F} = -\nabla\phi - c^{-1}\partial_t\boldsymbol{A} + c^{-1}\boldsymbol{v}\times\nabla\times\boldsymbol{A}$$
$$\Delta\phi = -4\pi e\int f\, d^3\boldsymbol{v} - c^{-1}\nabla\cdot\partial_t\boldsymbol{A}$$
$$c\nabla\times\nabla\times\boldsymbol{A} = 4\pi\int \boldsymbol{v}\, f d^3\boldsymbol{v} - \nabla\partial_t\phi$$

Fast-slow maps = discrete-time fast-slow systems

Definition 2: (fast-slow map)

A **fast-slow map** on $X \times Y \ni (x, y)$ is a family of mappings

$$F_\gamma : X \times Y \to X \times Y : (x, y) \mapsto (\psi_\gamma(x, y), \Psi_\gamma(x, y))$$

with vector parameter γ such that

$$F_0(x, y) = (x, \Psi_0(x, y)),$$

and

- For each $x \in X$ there is a unique $y = y_0^*(x)$ that solves $\Psi_0(x, y) = y$
- The linear map $D_y\Psi_0(x, y_0^*(x)) - 1 : Y \to Y$ is invertible

J. W. Burby and T. J. Klotz, *Commun. Nonlinear Sci.* **89**: 105289 (2020)

Discrete-time fast-slow structure $\Rightarrow$ discrete-time slow manifolds

Theorem 2: (existence of slow manifolds; discrete-time)

- For each fast-slow map there is a unique formal power series

$$y^*_\gamma(x) = y^*_0(x) + y^*_1[\gamma](x) + \epsilon^2\, y^*_2[\gamma,\gamma](x) + \ldots$$

  such that the graph $S_\gamma = \{(x,y) \mid y = y^*_\gamma(x)\}$ is an invariant manifold *to all orders in* γ.
- Equivalently, $y = y^*_\gamma(x)$ provides a formally-exact closure of the slow-variable map,

$$x \mapsto \psi_\gamma(x, y^*_\gamma(x))$$

Slow manifold reduction of the fast-slow map

J. W. Burby and T. J. Klotz, *Commun. Nonlinear Sci.* **89**: 105289 (2020)

Example 1:

- Variational IMEX discretization of Vlasov-Maxwell defines fast-slow map for $\epsilon \ll h \ll 1$. Discrete-time slow manifold recovers:
  - 0^{th}-order in ϵ: 2^{nd}-order scheme for Vlasov-Poisson
  - 1^{st}-order in ϵ: 2^{nd}-order scheme for for Vlasov-Darwin

$$
\begin{aligned}
\boldsymbol{E}_\gamma^{T*} &= -\frac{(h\,\delta)^2}{c^2}\Delta_1^{-1}\Pi_1^T \sum_a \frac{4\pi e_a^2}{m_a} I_1^* \left(I_1(\boldsymbol{E}^L) * S_{\boldsymbol{x}_a} S_{\boldsymbol{x}_a} \right) \\
&\quad + \frac{(h\,\delta)^2}{c^2}\Delta_1^{-1}\Pi_1^T \sum_a 4\pi e_a I_1^* \left(\nabla \cdot [\boldsymbol{v}_a \boldsymbol{v}_a S_{\boldsymbol{x}_a}]\right) + O(\gamma^5) \\
\boldsymbol{B}_\gamma^* &= (h\,\delta)\frac{4\pi}{c}\Delta_2^{-1}\mathbf{d}_1 \sum_a e_a I_1^* \left(\boldsymbol{v}_a S_{\boldsymbol{x}_a}\right) + O(\gamma^3)
\end{aligned}
$$

J. W. Burby, APS-DPP Poster, (2019), http://meetings.aps.org/link/BAPS.2019.DPP.CP10.15, LA-UR-19-30654

c$^{\text{ts}}$-time slow manifold

$$\boldsymbol{E}_{\epsilon}^{T*} = \frac{\epsilon^2}{c^2}\nabla^{-2}\Pi^T\sum_{\sigma}\frac{4\pi e^2 n_\sigma}{m_\sigma}\boldsymbol{E}^L - \frac{\epsilon^2}{c^2}\nabla^{-2}\Pi^T\sum_{\sigma}4\pi e_\sigma\nabla\cdot\int \boldsymbol{v}\boldsymbol{v}\, f_\sigma\, d^3\boldsymbol{v} + O(\epsilon^3)$$

$$\boldsymbol{B}_{\epsilon}^{*} = -\epsilon\,\frac{4\pi}{c}\nabla^{-2}\nabla\times\sum_{\sigma}e_\sigma\int \boldsymbol{v}\, f_\sigma\, d^3\boldsymbol{v} + O(\epsilon^2)$$

Discrete-time slow manifold

$$\boldsymbol{E}_{\gamma}^{T*} = -\frac{(h\,\delta)^2}{c^2}\Delta_1^{-1}\Pi_1^T\sum_a\frac{4\pi e_a^2}{m_a}I_1^*\left(I_1(\boldsymbol{E}^L)*S_{\boldsymbol{x}_a}\,S_{\boldsymbol{x}_a}\right) + \frac{(h\,\delta)^2}{c^2}\Delta_1^{-1}\Pi_1^T\sum_a 4\pi e_a I_1^*\left(\nabla\cdot[\boldsymbol{v}_a\boldsymbol{v}_a\,S_{\boldsymbol{x}_a}]\right) + O(\gamma^5)$$

$$\boldsymbol{B}_{\gamma}^{*} = (h\,\delta)\frac{4\pi}{c}\Delta_2^{-1}\mathbf{d}_1\sum_a e_a\, I_1^*\left(\boldsymbol{v}_a\,S_{\boldsymbol{x}_a}\right) + O(\gamma^3)$$

Example 2:

Lorentz loop dynamics

Phase space loop of magnetized charged particles evolves according to

$$\partial_t \tilde{\boldsymbol{v}}(\theta, t) + \frac{1}{\epsilon}|\boldsymbol{B}(\overline{\boldsymbol{x}}(t))|\,\partial_\theta \tilde{\boldsymbol{v}}(\theta, t) = \frac{1}{\epsilon}\tilde{\boldsymbol{v}}(\theta, t) \times \boldsymbol{B}(\tilde{\boldsymbol{x}}(\theta, t))$$

$$\partial_t \tilde{\boldsymbol{x}}(\theta, t) + \frac{1}{\epsilon}|\boldsymbol{B}(\overline{\boldsymbol{x}}(t))|\,\partial_\theta \tilde{\boldsymbol{x}}(\theta, t) = \tilde{\boldsymbol{v}}(\theta, t)$$

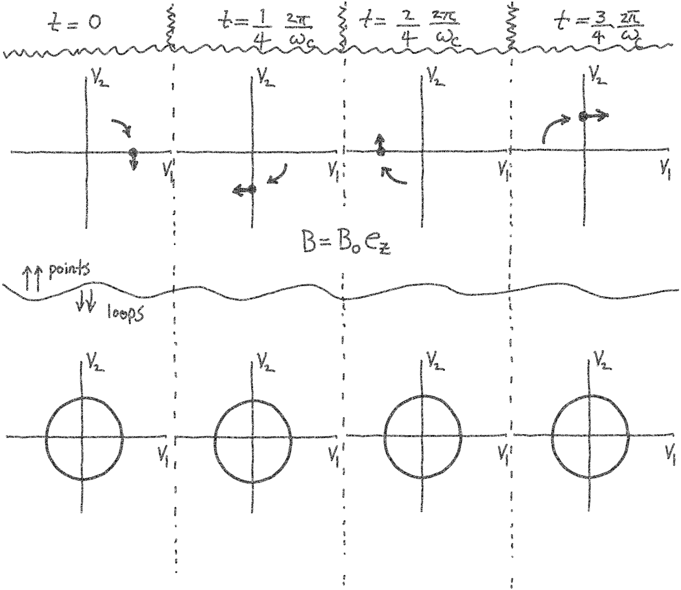

t = 0
t = 1/4 2π/ω_c
t = 2/4 2π/ω_c
t = 3/4 2π/ω_c
v_2
v_1
B = B_0 e_z
points
loops

Proposition:

Phase space loop dynamics is a fast-slow system.

Theorem:

Slow manifold reduction of loop dynamics, $\dot{x} = g_\epsilon(x, y_\epsilon^*(x))$, describes the dynamics of a single *guiding center*

$$\dot{\boldsymbol{x}} = \overline{u}\boldsymbol{b} - \epsilon \underbrace{\frac{(\mu_0 \nabla|\boldsymbol{B}| + \boldsymbol{b}\cdot\nabla\boldsymbol{b}) \times \boldsymbol{b}}{|\boldsymbol{B}|}}_{\nabla B \text{ and curvature drifts}} + O(\epsilon^2)$$

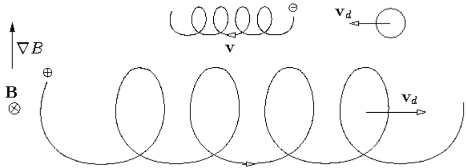

J. W. Burby, "Guiding center dynamics as motion on a formal slow manifold in loop space," *J. Math. Phys.* **61**:012703 (2020)

Example 2:

- Implicit midpoint for Lorentz loop dynamics defines fast-slow map for $h \gg 2\pi/\omega_c$:
  - discrete-time slow manifold recovers integrator for guiding center dynamics

∇B-dominant $\Rightarrow$ ccw azimutal motion

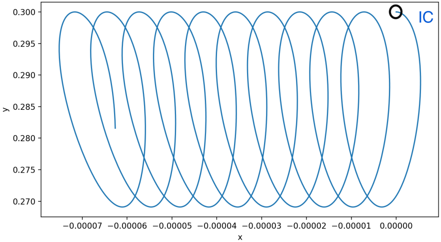

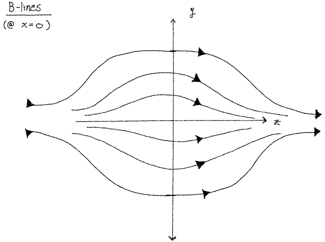

$$\text{IC: } (\overline{x}, \overline{y}, \overline{z}, \overline{u}, w_1, w_2) = (0, .3, 0, 1, 2, 0)$$
$$h = .5 \times 10^{-2} \quad \epsilon = 10^{-4}$$

J. W. Burby, "Integrating guiding center motion in loop space," Courant Institute Invited Talk: LA-UR-19-2276 (2019)

Example 2:

Lorentz-Pauli dynamics

The Lorentz-Pauli system is the ODE

$$\dot{\boldsymbol{v}} = -\mu\nabla|\boldsymbol{B}| + \frac{1}{\epsilon}\boldsymbol{v}\times\boldsymbol{B}(\boldsymbol{x})$$
$$\dot{\boldsymbol{x}} = \boldsymbol{v}$$

where $\mu > 0$ is a parameter.

Proposition: (Xiao-Qin)

The Lorentz-Pauli system is fast-slow. The slow manifold reduction recovers guiding center dynamics with magnetic moment μ.

J. Xiao and H. Qin, "Slow manifolds of classical Pauli particle enable structure-preserving geometric algorithms for guiding center dynamics," *Comp. Phys. Commun.* **265**:107981 (2021)

Proposition:

Boris discretization of Lorentz-Pauli defines a fast-slow map for $\epsilon \ll h \ll 1$. ($\delta = \epsilon/h$.)

$$\delta(\boldsymbol{v}_{k+1/2} - \boldsymbol{v}_{k-1/2}) = \frac{1}{2}(\boldsymbol{v}_{k+1/2} + \boldsymbol{v}_{k-1/2}) \times \boldsymbol{B}(\boldsymbol{x}_k)$$
$$(\boldsymbol{x}_k - \boldsymbol{x}_{k-1}) = h\, \boldsymbol{v}_{k-1/2}$$

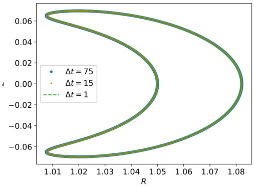

The numerical experiments are in the simplified tokamak field as described in Ref. [2]. The potentials are

$$\mathbf{A}\,(x, y, z) = \frac{1}{2} B_0 \left(\frac{r^2}{2R} \mathbf{e}_\xi - \log(R)\mathbf{e}_z + \frac{z}{2R}\mathbf{e}_R \right), \quad (18)$$
$$\phi\,(x, y, z) = 0\,, \quad (19)$$

where

$$R = r\sqrt{x^2 + y^2}\,, r = \sqrt{(R-1)^2 + z^2}\,, \quad (20)$$
$$\mathbf{e}_\xi = \mathbf{e}_R[-\frac{y}{R}, \frac{x}{R}, 0]\,, \mathbf{e}_R = [\frac{x}{R}, \frac{y}{R}, 0]\,, \quad (21)$$

J. Xiao and H. Qin, "Slow manifolds of classical Pauli particle enable structure-preserving geometric algorithms for guiding center dynamics," *Comp. Phys. Commun.* **265**:107981 (2021)

Xiao-Qin integrator performance in realistic fields

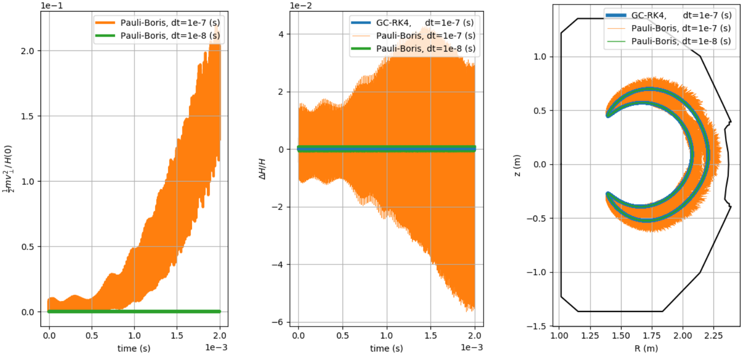

$T_c = 3.14 \times 10^{-8}$. DIII-D shot 66832 at 2384 ms

Part 2: nearly-periodic maps

Nearly-periodic systems limit to periodic flows

Definition 3: (nearly-periodic system)

An ODE $\dot{z} = V_\epsilon(z)$ is a **nearly-periodic system** if

- $V_\epsilon(z)$ is smooth in (z, ϵ)
- Each trajectory of $\dot{z} = V_0(z)$ is periodic with nowhere-vanishing angular frequency $\omega_0(z)$

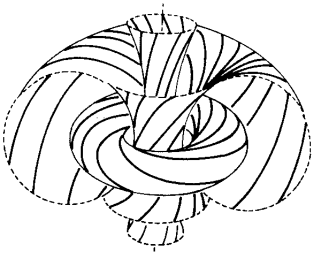

Nearly-periodic systems limit to periodic flows

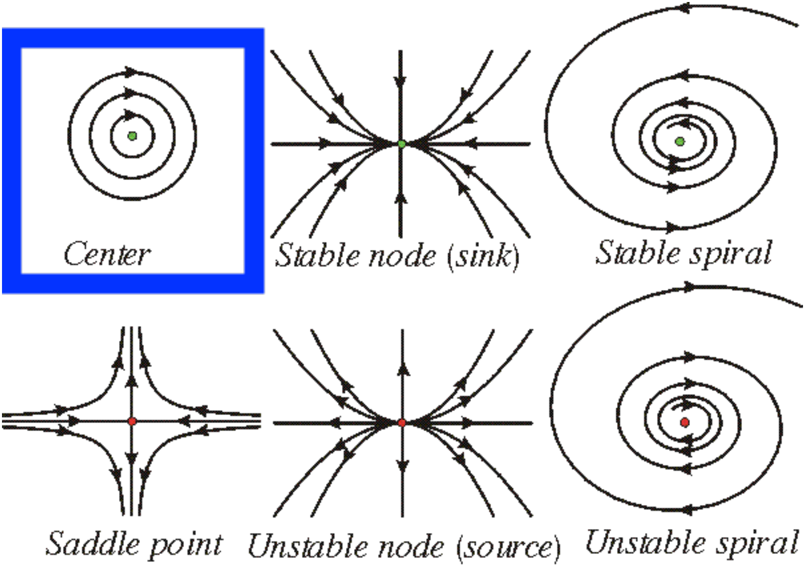

nearly-periodic structure $\Rightarrow$ existence of $U(1)$-symmetry

Theorem 3: (all-orders $U(1)$ symmetry)

Each nearly-periodic system admits a formal $U(1)$-symmetry. Equivalently, there is a power series vector field $R_\epsilon = R_0 + \epsilon\, R_1 + \dots$ such that

- $R_0 = V_0/\omega_0$
- $[R_\epsilon, V_\epsilon] = 0$ to all-orders in ϵ
- $\exp(2\pi \mathcal{L}_{R_\epsilon}) = \text{id}$

R_ϵ is called the **roto-rate**. It is unique!

M. Kruskal, "Asymptotic theory of Hamiltonian and other systems with all solutions nearly periodic," *J. Math. Phys.* **3**: 806 (1962)

nearly-periodic structure $\Rightarrow$ existence of $U(1)$-symmetry

Corollary: (adiabatic invariance)

If a nearly-periodic system $\dot{z} = V_\epsilon(z)$ is also Hamiltonian, then it admits an adiabatic invariant. Equivalently, there exists a power-series scalar function $\mu_\epsilon = \mu_0 + \epsilon\,\mu_1 + \dots$ such that

$$\mathcal{L}_{V_\epsilon}\mu_\epsilon = 0$$

to all-orders in ϵ.

M. Kruskal, "Asymptotic theory of Hamiltonian and other systems with all solutions nearly periodic," *J. Math. Phys.* **3**: 806 (1962).

J. W. Burby and J. Squire, "General formulas for adiabatic invariants in nearly periodic Hamiltonian systems," *J. Plasma Phys.* **86**: 835860601 (2020).

Example:

Proper-time Lorentz force dynamics

A magnetized charged particle's 4-position R and 4-velocity V evolve according to

$$\frac{dV}{d\tau} = \boldsymbol{F}(R)\, V, \quad \frac{dR}{d\tau} = \epsilon\, V,$$

where τ is the proper time and $\boldsymbol{F}$ is the Faraday tensor.

Proposition:

Proper-time Lorentz force dynamics is nearly periodic. The limiting flow map is

$$(R, V) \mapsto (R, P_{\|} V + [\cos\theta + \sin\theta\, \boldsymbol{F}_0/\omega_0] P_{\perp}\, V)$$

where $\omega_0 = \sqrt{-\mathrm{tr}(\boldsymbol{F}_0^2)/2}$ and $\theta = \tau\omega_0$.

J. W. Burby and E. Hirvijoki, "Normal stability of slow manifolds in nearly-periodic Hamiltonian systems," *J. Math. Phys.* (2021, **submitted**, arXiv:2104.02190)

Nearly-periodic maps limit to rotations along circles

Definition 4: (nearly-periodic map)

A mapping $F_\gamma : Z \to Z$ with vector parameter γ is a **nearly-periodic map** if there is a $U(1)$-action $\Phi_\theta : Z \to Z$ and an angle $\theta_0 \in U(1)$ such that

$$F_0 = \Phi_{\theta_0}.$$

If $\theta_0/(2\pi)$ is rational, F_γ is **resonant**. Otherwise it is **non-resonant**.

$$\theta \mapsto \theta + \theta_0$$

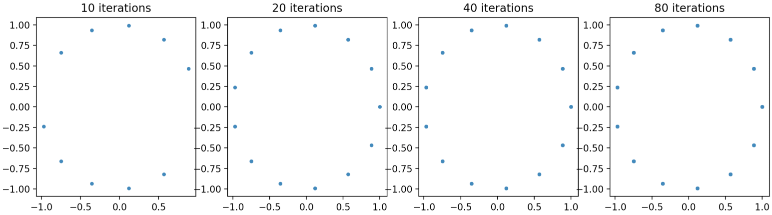

$$\theta_0 = 2\pi(7/13)$$

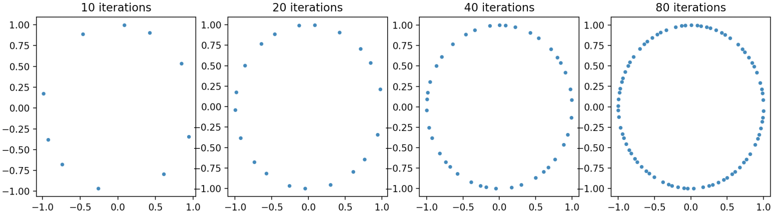

$$\theta_0 = 2\pi\phi$$

Discrete nearly-periodic structure $\Rightarrow$ discrete-time $U(1)$ symmetry

Theorem 4: (discrete-time all-orders $U(1)$ symmetry)

Each non-resonant nearly-periodic map F_γ admits a formal $U(1)$ symmetry. Equivalently, there exists a power-series vector field $R_\epsilon = R_0 + R_1[\gamma] + R_2[\gamma,\gamma] + \dots$ such that

- $R_0 = \partial_\theta \Phi_\theta \mid_{\theta=0}$
- $F_\gamma^* R_\gamma = R_\gamma$
- $\exp(2\pi \mathcal{L}_{R_\gamma}) = \mathrm{id}$

Discrete nearly-periodic structure $\Rightarrow$ discrete-time $U(1)$ symmetry

Corollary: (discrete-time adiabatic invariance)

If a non-resonant nearly-periodic map is also Hamiltonian* then it admits an adiabatic invariant. Equivalently, there exists a power series scalar function $\mu_\gamma = \mu_0 + \mu_1[\gamma] + \mu_2[\gamma,\gamma] + \dots$ such that

$$\mu_\gamma(F_\gamma(z)) - \mu_\gamma(z) = 0$$

to all orders in γ for each $z \in Z$.

Part III: Application to symplectic integration

Symplectic integration preserves the geometry of phase space for non-dissipative systems

$$\dot{p} = -\partial_q H, \quad \dot{q} = \partial_p H$$

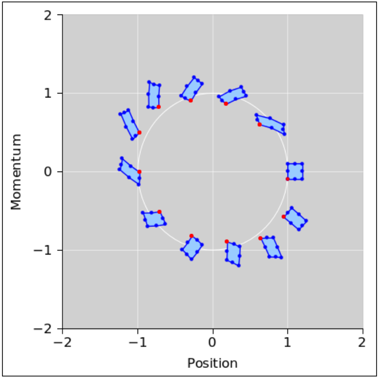

Phase space geometry $=$ symplectic 2-form

$$dq_{k+1} \wedge dp_{k+1} = dq_k \wedge dp_k$$

Symplectic integration preserves the geometry of phase space for non-dissipative systems

Benefits of symplectic integration

- numerical stability for many timesteps *without introducing dissipation*
- Noether's theorem in discrete time
- reveals useful mechanisms that can be ported into non-symplectic schemes
  - e.g. Villasenor-Buneman current deposition for PIC emerges naturally from symplectic PIC.
  - This provides easy way to generalize V-B to irregular meshes, higher-order finite elements, non-trivial particle shape functions, **even drift kinetics**

Canonical symplectic integration is routine

$$\dot{p} = -\partial_q H, \quad \dot{q} = \partial_p H$$

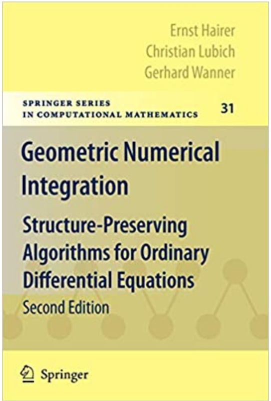

Famous example: Leapfrog

$$H(q, p) = \frac{1}{2}|p|^2 + V(q)$$

$$q_{k+1} = q_k + h\, p_{k+1/2}$$

$$p_{k+3/2} = q_{k+1/2} - h\, \partial_q V(q_{k+1})$$

Symplectic integration methods can also be used to build **symplectic neural networks**

J. W. Burby, Q. Tang, R. Maulik, "Fast neural Poincaré maps for toroidal magnetic fields," *Plasma. Phys. Control. Fusion* **63**: 024001 (2021)

But non-canonical symplectic integration is notoriously difficult

Non-canonical Hamiltonian systems

$$\dot{z}^i \omega_{ij}(z) = \partial_j H(z), \quad \omega_{ij} = -\omega_{ji}, \quad \partial_i \omega_{jk} + \partial_j \omega_{ki} + \partial_k \omega_{ij} = 0$$

canonical symplectic property

$$dq_{k+1} \wedge dp_{k+1} \\ = dq_k \wedge dp_k$$

non-canonical symplectic property

$$\omega_{ij}(z_{k+1}) dz^i_{k+1} \wedge dz^j_{k+1} \\ = \omega_{ij}(z_k) dz^i_k \wedge dz^j_k$$

But non-canonical symplectic integration is notoriously difficult

Degenerate variational integrators for magnetic field line flow and guiding center trajectories

Physics of Plasmas 25, 052502 (2018); https://doi.org/10.1063/1.5022277

C. L. Ellison[1,2,a)], J. M. Finn[3,b)], J. W. Burby[4], M. Kraus[5], H. Qin[2,6], *and* W. M. Tang[2]

View Affiliations

PDF CHORUS ABSTRACT FULL TEXT FIGURES CITED BY TOOLS SHARE METRICS

TOPICS

- Partial differential equations
- Plasma dynamics
- Hamiltonian mechanics
- Differentiable manifold
- Recurrence relations
- Magnetic potential
- Plasma physics
- Dynamical systems
- Integral calculus
- Vector fields

ABSTRACT

Symplectic integrators offer many benefits for numerically approximating solutions to Hamiltonian differential equations, including bounded energy error and the preservation of invariant sets. Two important Hamiltonian systems encountered in plasma physics–the flow of magnetic field lines and the guiding center motion of magnetized charged particles–resist symplectic integration by conventional means because the dynamics are most naturally formulated in non-canonical coordinates. New algorithms were recently developed using the variational integration formalism; however, those integrators were found to admit parasitic mode instabilities due to their multistep character. This work eliminates the multistep character, and therefore the parasitic mode instabilities via an adaptation of the variational integration formalism that we deem "degenerate variational integration." Both the

- Techniques for building canonical symplectic schemes **double dimension of phase space** when applied to non-canonical systems
- BIG PROBLEM: extra dimensions $\Rightarrow$ numerical instabilities generically
- OPEN QUESTION: Can these instabilities be eliminated?

But non-canonical symplectic integration is notoriously difficult

Examples:

- Guiding center dynamics
- (collisionles) Vlasov-Maxwell
- various forms of MHD
- MANY MORE!

These instabilities = drift away from discrete-time slow manifold

Example: "non-canonical pendulum"

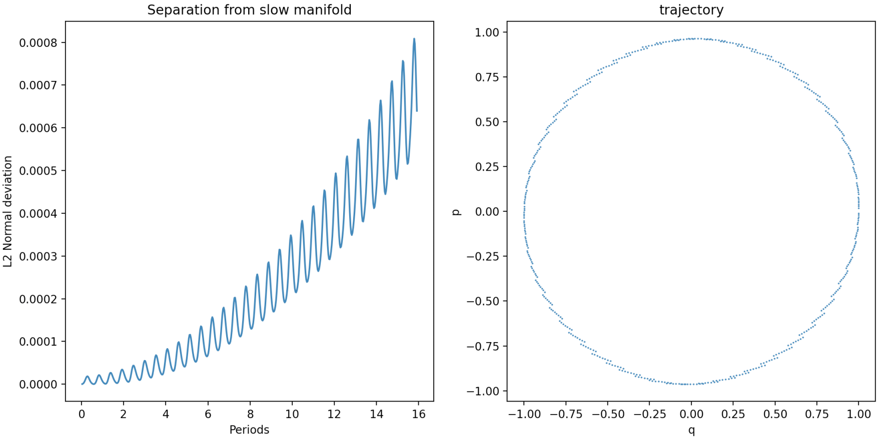

C. L. Ellison *et al.* *Phys. Plasmas* **25**: 052502 (2018).

These instabilities = drift away from discrete-time slow manifold

Example: “non-canonical pendulum”

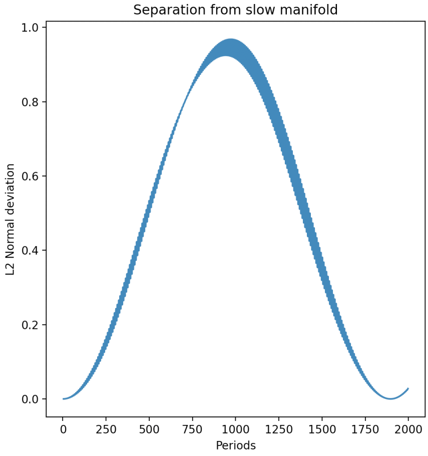

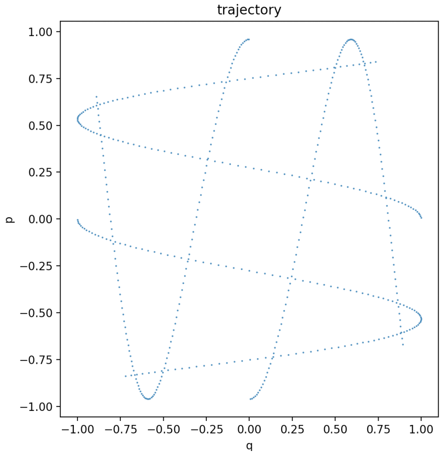

C. L. Ellison *et al.* *Phys. Plasmas* **25**: 052502 (2018).

Instabilities can be eliminated using nearly-periodic maps!

Theorem:

The generating function

$$S(q,\overline{q}) = -\hbar H + \hbar\,\delta\,\langle X_H, \overline{z} - z\rangle - \frac{1}{2}\hbar^2\,\delta\,\langle X_H, X_H\rangle + \int_z^{\overline{z}} \vartheta - \frac{1}{4}\left(\frac{\sin\theta_0}{1-\cos\theta_0}\right)\langle \overline{z} - z - \hbar X_H, \overline{z} - z - \hbar X_H\rangle$$

defines a Hamiltonian nearly-periodic map on $(z,\dot{z})$-space. On the zero level set $\mu_\gamma = 0$, the map induces a non-canonical symplectic integrator for the non-canonical Hamiltonian system $\dot{z} = X_H(z)$. **Normal instabilities are impossible by discrete-time adiabatic invariance.**

Instabilities can be eliminated using nearly-periodic maps!

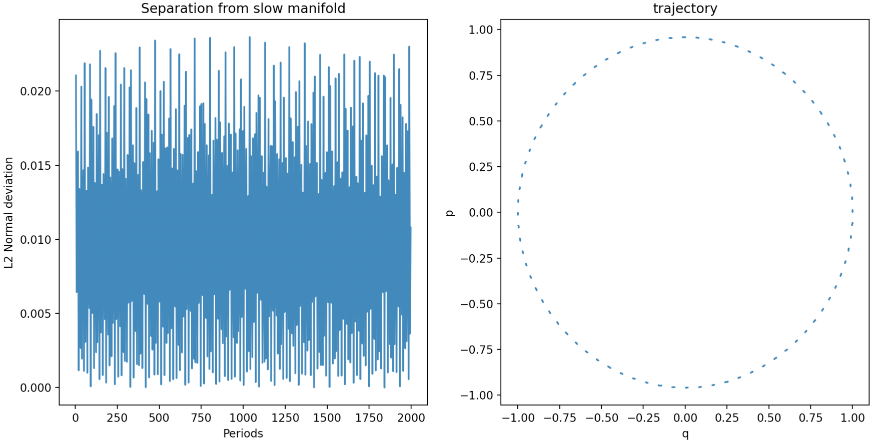

Thank you!

Bibliography

1 G. Miloshevich and **J. W. Burby**, "Hamiltonian reduction of Vlasov-Maxwell to a dark slow manifold," *J. Plasma Phys.* [submitted, arXiv:2104.03092] (2021)

2 **J. W. Burby** and E. Hirvijoki, "Normal stability of slow manifolds in nearly-periodic Hamiltonian systems," *J. Math. Phys.* [submitted, arXiv:2104.02190] (2021)

3 J. Xiao and H. Qin, "Slow manifolds of classical Pauli particle enable structure-preserving geometric algorithms for guiding center dynamics," *Comp. Phys. Commun.* **265**:107981 (2021)

4 **J. W. Burby** and J. Squire, "General formulas for adiabatic invariants in nearly periodic Hamiltonian systems," *J. Plasma Phys.* **86**: 835860601 (2020)

5 **J. W. Burby**, Q. Tang, and R. Maulik, "Fast neural Poincaré maps for toroidal magnetic fields," *Plasma Phys. Control. Fusion* **63**: 024001 (2020)

6 **J. W. Burby** and T. J. Klotz, "Slow manifold reduction for plasma science," *Commun. Nonlinear Sci. Numer. Simul.* **89**: 105289 (2020)

7 **J. W. Burby** and D. E. Ruiz, "Variational nonlinear WKB in the Eulerian frame," *J. Math. Phys.* **61**: 053101 (2020)

8 **J. W. Burby**, "Guiding center dynamics as motion on a formal slow manifold in loop space," *J. Math. Phys.* **61**: 012703 (2020)

9 C. L. Ellison, J. M. Finn, **J. W. Burby**, M. Kraus, H. Qin, W. M. Tang , "Degenerate variational integrators for magnetic field line flow and guiding center trajectories," *Phys. Plasmas* **25**:052502 (2018)

10 **J. W. Burby**, APS-DPP Poster, http://meetings.aps.org/link/BAPS.2019.DPP.CP10.15, LA-UR-19-30654, (2019)

11 **J. W. Burby**, "Integrating guiding center motion in loop space," Courant Institute Invited Talk: LA-UR-19-2276 (2019)

12 **J. W. Burby** and W. Sengupta, "Hamiltonian structure of the guiding center plasma model," *Phys. Plasmas* **25**:020703 (2018)

13 **J. W. Burby**, "Magnetohydrodynamic motion of a two-fluid plasma," *Phys. Plasmas* **24**:082104 (2017)

14 M. Kruskal, "Asymptotic theory of Hamiltonian and other systems with all solutions nearly periodic," *J. Math. Phys.* **3**: 806 (1962)